6-1-2023

The sphingolipids ceramide and inositol phosphorylceramide protect the Leishmania major membrane from sterol-specific toxins

Chaitanya S Haram
Texas Tech University

Samrat Moitra
Texas Tech University

Rilee Keane
Texas Tech University

F Matthew Kuhlmann
Washington University School of Medicine in St. Louis

Cheryl Frankfater
Washington University School of Medicine in St. Louis

See next page for additional authors

Recommended Citation

Haram, Chaitanya S; Moitra, Samrat; Keane, Rilee; Kuhlmann, F Matthew; Frankfater, Cheryl; Hsu, Fong-Fu; Beverley, Stephen M; Zhang, Kai; and Keyel, Peter A, "The sphingolipids ceramide and inositol phosphorylceramide protect the Leishmania major membrane from sterol-specific toxins." Journal of Biological Chemistry. 299, 6. 104745 (2023).
https://digitalcommons.wustl.edu/oa_4/2663

Authors

Chaitanya S Haram, Samrat Moitra, Rilee Keane, F Matthew Kuhlmann, Cheryl Frankfater, Fong-Fu Hsu, Stephen M Beverley, Kai Zhang, and Peter A Keyel

The sphingolipids ceramide and inositol phosphorylceramide protect the *Leishmania major* membrane from sterol-specific toxins

Chaitanya S. Haram[1,‡], Samrat Moitra[1,‡], Rilee Keane[1], F. Matthew Kuhlmann[2], Cheryl Frankfater[3], Fong-Fu Hsu[3], Stephen M. Beverley[2], Kai Zhang[1], and Peter A. Keyel[1,*]

From the [1]Department of Biological Sciences, Texas Tech University, Lubbock, Texas, USA; [2]Department of Molecular Microbiology, and [3]Division of Endocrinology, Metabolism, and Lipid Research, Department of Medicine, Mass Spectrometry Resource, Washington University School of Medicine, St Louis, Missouri, USA

The accessibility of sterols in mammalian cells to exogenous sterol-binding agents has been well-described previously, but sterol accessibility in distantly related protozoa is unclear. The human pathogen *Leishmania major* uses sterols and sphingolipids distinct from those used in mammals. Sterols in mammalian cells can be sheltered from sterol-binding agents by membrane components, including sphingolipids, but the surface exposure of ergosterol in *Leishmania* remains unknown. Here, we used flow cytometry to test the ability of the *L. major* sphingolipids inositol phosphorylceramide (IPC) and ceramide to shelter ergosterol by preventing binding of the sterol-specific toxins streptolysin O and perfringolysin O and subsequent cytotoxicity. In contrast to mammalian systems, we found that *Leishmania* sphingolipids did not preclude toxin binding to sterols in the membrane. However, we show that IPC reduced cytotoxicity and that ceramide reduced perfringolysin O- but not streptolysin O-mediated cytotoxicity in cells. Furthermore, we demonstrate ceramide sensing was controlled by the toxin L3 loop, and that ceramide was sufficient to protect *L. major* promastigotes from the antileishmaniasis drug amphotericin B. Based on these results, we propose a mechanism whereby pore-forming toxins engage additional lipids like ceramide to determine the optimal environment to sustain pore formation. Thus, *L. major* could serve as a genetically tractable protozoan model organism for understanding toxin-membrane interactions.

Annually, 1.5 to 2 million cases and 70,000 deaths are caused by the neglected tropical disease, leishmaniasis. Leishmaniasis is caused by parasites in the genus *Leishmania*. In contrast to mammals, these parasites use ergosterol instead of cholesterol and distinct sphingolipids. These lipids represent a therapeutic target for *Leishmania*, exemplified by the first-line treatment liposomal amphotericin B, which binds to membrane ergosterol and induces pores in the membrane (1). However, the lipid environment enabling access of amphotericin B and other sterol-binding agents to the membrane is unknown. Resistance to amphotericin B is described for lab strains (2), and amphotericin B has nephrotoxic side effects (3, 4), highlighting the need to understand the impact of the lipid environment. In order to achieve this goal, it is critical to understand the determinants that control sterol access.

Membrane sterol access is primarily controlled by sphingolipids in mammalian cells. In mammalian cells, plasma membrane cholesterol is evenly split between sphingomyelin-cholesterol complexes, other "inaccessible" cholesterol, and "accessible" cholesterol (5). Accessible cholesterol is defined by the ability of the membrane cholesterol to bind to exogenous sterol-binding agents, like cholesterol-dependent cytolysins (CDCs) (5). Sphingomyelinases liberate cholesterol from cholesterol–sphingomyelin complexes, increasing sterol sensitivity to CDCs (6). Thus, sphingolipids are a prominent factor governing sterol accessibility in mammalian cells.

Compared to mammalian cells, *Leishmania* synthesizes different lipids, which could alter sterol accessibility. Like cholesterol, ergosterol forms detergent resistant microdomains with the primary *Leishmania* sphingolipid, inositol phosphorylceramide (IPC), and GPI-anchored proteins like gp63 (7). IPC comprises 10% of the total lipids in *Leishmania major* (8). Manipulation of IPC is best controlled at the level of its synthesis instead of cleavage. IPC is not cleaved by *B. cereus* sphingomyelinase, and the lipase that cleaves IPC (9) likely cleaves other lipids, complicating the interpretation of any results using enzymes. Detection of IPC requires mass spectrometry approaches because it is not recognized by the animal sphingolipid sensors ostreolysin A or lysenin (10, 11). Two key enzymes affecting IPC are serine palmitoyl transferase (SPT), the first committed step of sphingolipid synthesis, and IPC synthase (IPCS). Genetic ablation of the second subunit of SPT (*SPT2*) inactivates the enzyme. Knockout of *SPT2* prevents the formation of sphingosine, which leads to defects in ceramide and IPC synthesis and infectivity but normal promastigote growth in the logarithmic phase (7). Similar results are observed when SPT2 is chemically inhibited with the drug myriocin (7). Similarly, genetic deletion of *IPCS* completely depletes IPC without impacting parasite growth or virulence

---

(12). These mutants retain upstream sphingolipids, including enhanced ceramide levels (12). Thus, both genetic and pharmacological tools exist to measure the control of *Leishmania* sphingolipids over ergosterol accessibility.

Sterol accessibility is measured using inactive CDCs from Gram-positive bacteria. *Streptococcus pyogenes* secretes the CDC Streptolysin O (SLO), while *Clostridium perfringens* secretes the CDC perfringolysin O (PFO) (13). These CDCs engage a range of sterols, including ergosterol (14). CDCs bind to sterol in the membrane, oligomerize and insert 20 to 30 nm pores into the membrane (13). One advantage of CDCs is that their properties can be changed using mutagenesis, which we and others have extensively characterized (15–21). Binding can be ablated by mutating two residues that drive sterol recognition (ΔCRM), or by introducing mutations that interfere with glycan binding (20). Similarly, mutation of two Gly to Val produces an inactive, non-toxic "monomer-locked" CDC that binds sterols (15, 17, 19). Finally, SLO and PFO engage sterols in distinct, but unknown, lipid environments (16, 18). SLO binds to and inserts into membranes faster than PFO (16, 18). The increased rate of binding and insertion is interpreted as SLO binding in a wider range of sterol microenvironments than PFO (16, 18). However, the identity of the microenvironment permissive for SLO or PFO remains unknown. The microenvironment requirements for each toxin can be switched to that of the other toxin by introducing point mutations in the membrane-binding L3 loop of the CDC (15, 16, 18). Thus, CDCs represent a versatile tool for probing the membrane environment and accessibility of sterols, such as the ergosterol environment in *Leishmania*.

Here, we tested the hypothesis that *Leishmania* shields the ergosterol target of amphotericin B in a manner similar to sterol shielding by mammalian cells. Surprisingly, we found that in contrast to mammalian cells, *Leishmania* sphingolipids did not prevent CDC binding, yet were able to prevent CDC cytotoxicity. Ceramide more strongly reduced PFO cytotoxicity, suggesting the mechanism of pore formation involves sensing ceramide *via* the L3 loop. Ceramide similarly contributed to the protection of *L. major* promastigotes from amphotericin B. Targeting ceramide and IPC may enhance ergosterol-targeting anti-leishmanial drugs.

Results

Sphingolipids do not limit accessible sterols in L. major

To determine if *L. major* sphingolipids shelter plasma membrane ergosterol, we measured the accessible ergosterol in wild-type (WT) and sphingolipid-deficient *L. major* promastigotes. We used fluorescently labeled "monomer-locked" (ML) SLO and PFO, which detect accessible cholesterol in mammalian cells (21). Both SLO ML and PFO ML exhibited dose-dependent binding to WT *L. major* (Fig. 1, *A* and *B*), indicating they can bind to ergosterol in the *Leishmania* plasma membrane. Surprisingly, the sphingolipid-null *spt2⁻* (7) showed no increase in SLO or PFO ML binding (Fig. 1, *A* and *B*). Overexpression of SPT2 in the *spt2⁻* background (*spt2⁻/+*SPT2) also did not change CDC binding (Fig. 1, *A* and

B). These data suggest that sphingolipids do not shelter ergosterol in *L. major*.

To confirm that sphingolipids do not shelter ergosterol in *L. major*, we used an *L. major* null mutant lacking the enzyme directly responsible for IPC synthesis from ceramide and phosphatidylinositol, *ipcs⁻*. Knockout of *IPCS* eliminates IPC but retains ceramide (12). To complement the knockout, episomal expression of IPCS in *ipcs⁻* cells (*ipcs⁻/+*IPCS) was used (12). Similar to *spt2⁻*, SLO ML and PFO ML binding of *ipcs⁻* was equivalent to wild type and *ipcs⁻/+*IPCS *L. major* (Fig. 1, *C* and *D*). Prior characterization of the *ipcs⁻* cells revealed an absence of IPC and accumulation of ceramide in the *ipcs⁻* cells, which was reverted by complementation (12). We conclude that neither ceramide (absent in *spt2⁻*) nor IPC (absent in both) alters ergosterol accessibility to CDCs in *L. major*.

While the CDCs can access ergosterol independent of sphingolipids, the amount of sterol and the extent of accessibility remain unclear. It was previously reported that *spt2⁻ L. major* promastigotes have reduced ergosterol, but increased cholesterol levels (22). To determine if interference in sphingolipid synthesis altered *L. major* sterol metabolism, we measured total sterols from promastigotes by GC-MS. Promastigotes with inactivated *de novo* sphingolipid synthesis trended to an increase (30–100% more than WT control) in total sterols, but similar ergosterol and ergosterol isomer (like 5-dehydroepisterol) levels (Fig. 1*E* and Table 1). The sterol increase came from cholesterol (taken up from the media) and sterol biosynthetic intermediates (Fig. 1*E* and Table 1). To compare the extent of CDC binding between *L. major* and mammalian cells, we challenged both HeLa cells and *L. major* promastigotes with fluorescent SLO ML. Compared to HeLa cells, promastigotes are poorly bound to SLO (Fig. 1*F*). To determine if this was due to the smaller surface area of *L. major* promastigotes, we normalized median fluorescence intensity (MFI) to surface area (Fig. S1*A*). When normalized to surface area, *L. major* bound more toxin per unit area than HeLa cells. Overall, these data suggest that CDCs sense ergosterol in *L. major* membrane independently of IPC or ceramide.

L. major sphingolipids limit CDC cytotoxicity

Since CDCs bind poorly to *L. major* regardless of the sphingolipid composition, we tested if the CDC binding was sufficient to promote cytotoxicity. We challenged log phase WT, *spt2⁻* or *spt2⁻/+*SPT2 promastigotes with SLO or PFO at 37 °C for 30 min. We found that SLO killed WT *L. major* only at very high doses but SLO killed *spt2⁻* promastigotes at ∼28-fold lower dose (Figs. 2*A*, S1, *B* and *C* and S2*A*). Although PFO did not kill WT or *spt2⁻/+*SPT2 promastigotes at any dose tested, it killed *spt2⁻* promastigotes like SLO (Figs. 2*B* and S2*B*). We next tested the *ipcs⁻* and *ipcs⁻/+*IPCS and found that *ipcs⁻* behaved similarly to *spt2⁻* (Fig. 2, *C* and *D* and S2, *C* and *D*). We determined the CDC concentration needed to kill 50% of the cells (LC₅₀) to compare the sensitivity of *spt2⁻* and *ipcs⁻ L. major*. To confirm our cytometry assay, we also
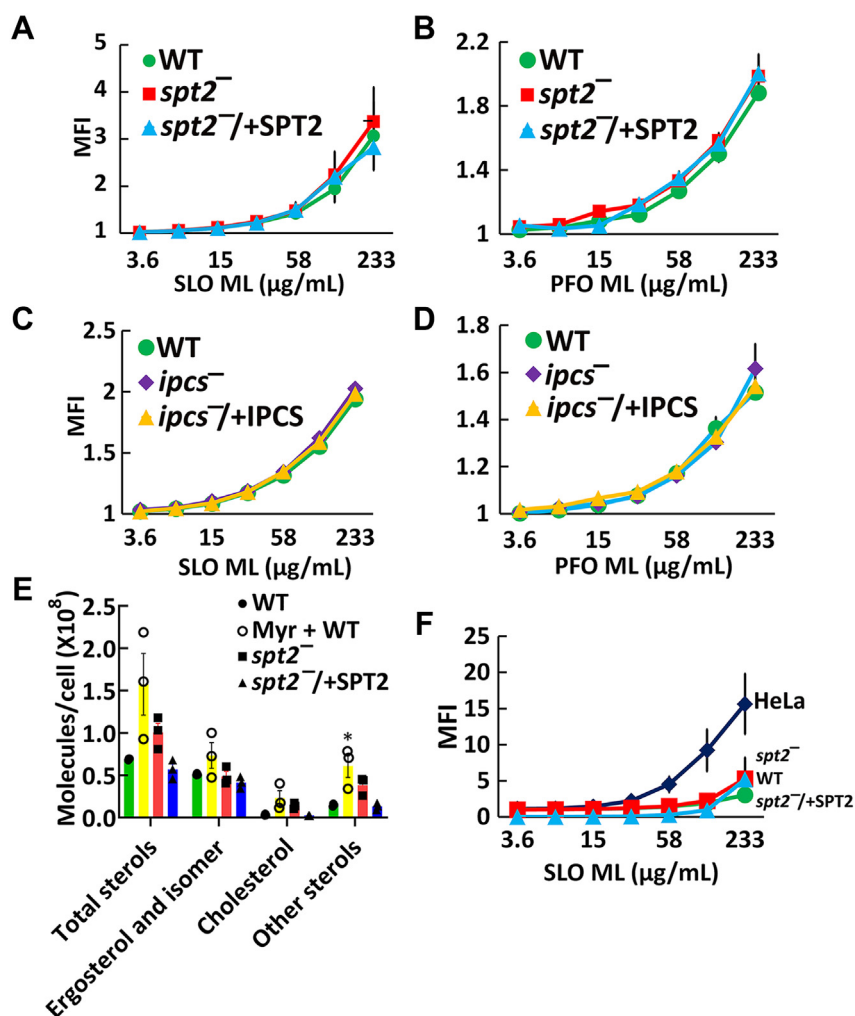
Figure 1. CDCs bind to *Leishmania major* promastigotes independently of sphingolipids. *A* and *B*, WT, *spt2⁻*, and *spt2⁻*/+SPT2, or (*C* and *D*) WT, *ipcs⁻*, and *ipcs⁻*/+IPCS *L. major* promastigotes were challenged with the indicated mass of (*A* and *C*) monomer-locked SLO (SLO ML) conjugated to Cy5 or (*B* and *D*) monomer-locked PFO (PFO ML) conjugated to Cy5 at 37 °C for 30 min and analyzed by flow cytometry. *E*, Total sterols from DMSO-treated WT, *spt2⁻*, and *spt2⁻*/+SPT2, or WT treated with 10 μM myriocin *L. major* promastigotes were extracted, derivatized and analyzed by GC-MS. *F*, HeLa cells or WT, *spt2⁻*, or *spt2⁻*/+SPT2 *L. major* promastigotes were challenged with SLO ML conjugated to Cy5 and analyzed by flow cytometry. Median Fluorescence Intensity ×10 (MFI) of Cy5 fluorescence gated on live cells is shown. Graphs display the mean ± SEM of three independent experiments. *p = 0.011 by one-way ANOVA with Tukey's multiple comparison post hoc testing (*A–D*, *F*). The x-axis is a $\log_2$ scale. WT, wild type.

performed an MTT assay. When killing was measured by MTT assay, we found similar results to our flow cytometry assay (Fig. S2*E*). This is consistent with our results in mammalian cells (15).

We next measured the LC_{50} for HeLa cells as a reference point because we have previously characterized cytotoxicity from CDCs in them (15, 21, 23, 24). Using HeLa cells as a reference point provides a relative estimate of how sensitive

Table 1
Sterols (×10⁷ molecules) present in *Leishmania major* promastigotes

Sterol	Elution time (min)	M/Z[a]	WT	Myriocin + WT	*spt2⁻*	*spt2⁻*/+SPT2
Cholesterol	15.533	458.4	0.330 ± 0.098	2.304 ± 1.528	1.375 ± 0.350	0.230 ± 0.026
Ergosterol	16.528	468.4	2.498 ± 0.250	3.476 ± 0.991	1.931 ± 0.533	1.979 ± 0.188
Ergosterol isomer	17.263	468.4	2.608 ± 0.142	3.860 ± 1.679	2.929 ± 0.508	2.165 ± 0.535
Cholesta-8,24-dien-3-ol (3β, 5α)	16.269	456.4	0.120 ± 0.042	0.537 ± 0.214	0.265 ± 0.066	0.136 ± 0.054
Cholesta-dien-3-ol[b]	15.968	456.4	0.151 ± 0.018	0.272 ± 0.109	0.177 ± 0.039	0.131 ± 0.026
Cholesta-dien-3-ol[b]	16.745	456.4	0.162 ± 0.041	0.676 ± 0.313	0.379 ± 0.243	0.156 ± 0.032
Ergostatetraenol[b]	16.003	466.4	0.090 ± 0.010	0.177 ± 0.063	0.102 ± 0.029	0.078 ± 0.013
Ergostatetraenol[b]	16.859	466.4	0.586 ± 0.071	1.541 ± 0.851	1.135 ± 0.168	0.417 ± 0.156
3-hydroxy ergosta 8,24(28) diene	17.025	470.4	0.132 ± 0.068	0.783 ± 0.207	0.579 ± 0.150	0.167 ± 0.104
Ergosta-7,22-dien-3-ol, (3β,22E)-?	17.522	470.4	0.234 ± 0.014	2.122 ± 0.987	1.207 ± 0.534	0.240 ± 0.077
Total sterols			6.91 ± 0.103	15.748 ± 6.301	10.077 ± 1.87	5.698 ± 1.118

[a] Trimethylsilyl derivatives.
[b] Positions of double bonds unknown.
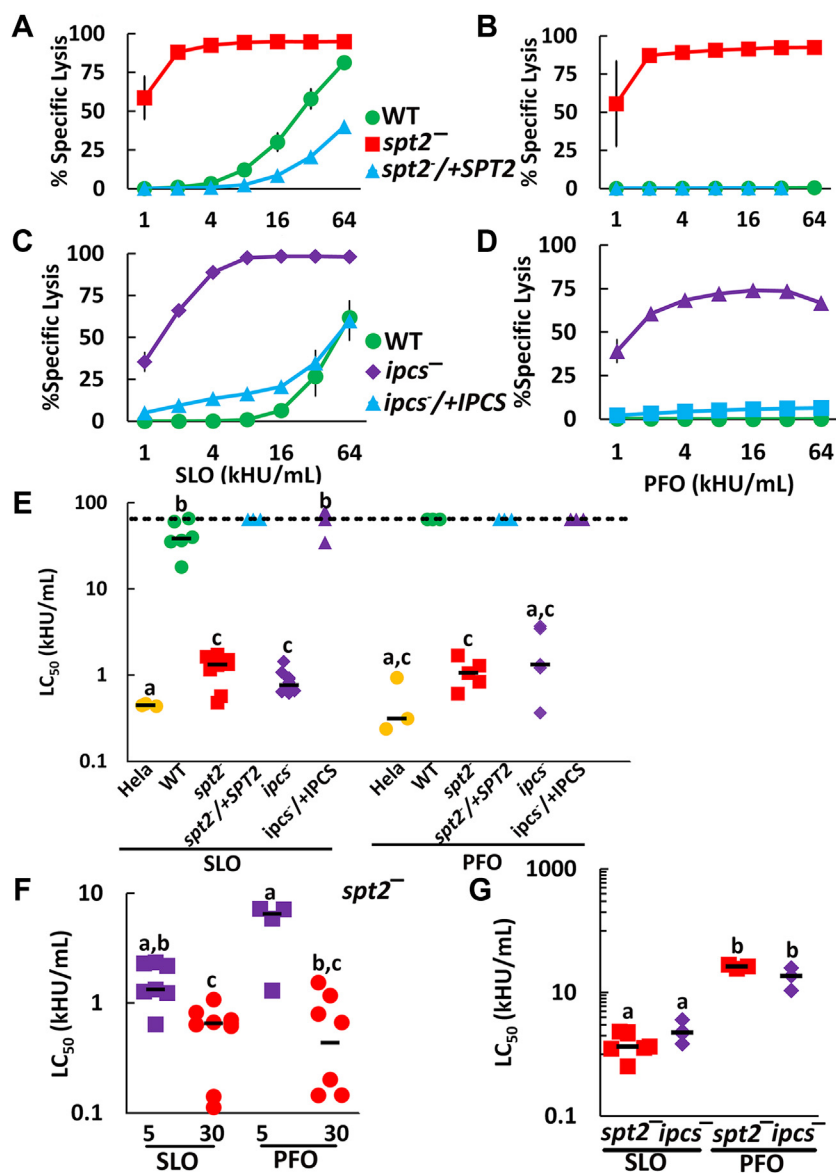
Figure 2. IPC protects *L. major* promastigotes from lysis by CDCs. *A* and *B*, WT, *spt2*⁻, and *spt2*⁻/+SPT2, or (*C* and *D*) WT, *ipcs*⁻, and *ipcs*⁻/+IPCS *L. major* promastigotes were challenged with (*A* and *C*) SLO or (*B* and *D*) PFO at the indicated concentrations for 30 min at 37 °C and PI uptake measured by flow cytometry. *E–G*, The LC$_{50}$ was calculated as described in the methods after challenging the indicated genotypes of *L. major* with 31 to 4000 HU/ml or HeLa cells with 32 to 2000 HU/ml of SLO or PFO for 30 min (*E* and *F*) or with 62 to 4000 HU/ml SLO or 1000 to 64,000 HU/ml PFO for 5 min (*F* and *G*) and measuring PI uptake by flow cytometry. *A–D*, Graphs display the mean ± SEM of at least three independent experiments. The dashed line indicates the highest concentration used. Points on this line had a LC$_{50}$ value ≥64,000 HU/ml. (*E–G*) Graphs display individual data points and median from at least three independent experiments. Statistical significance was determined by one-way ANOVA with Tukey post-testing. Groups sharing the same letter were not statistically different. For example, HeLa cells challenged with SLO (group a) were not statistically distinct from HeLa cells challenged with PFO, or *ipcs*⁻ cells challenged with PFO, but distinct from the remaining groups. In contrast, HeLa cells challenged with PFO (groups a and c), were only statistically distinct from WT and *ipcs*⁻/+IPCS *L. major* challenged with SLO (group b). (*A–D*) The x-axis is a log$_2$ scale. (*E–G*) The y-axis is a log$_{10}$ scale. PFO, perfringolysin O; SLO, Streptolysin O; WT, wild type.

L. major promastigotes become when they are sphingolipid deficient. We found that sphingolipid-deficient *L. major* remained 1.5 to 2 times more resistant than HeLa cells when challenged with either SLO or PFO (Figs. 2*E* and S2). Since sphingolipid-deficient *L. major* had elevated cholesterol levels, it is possible the sterol intermediates mediate the cytotoxicity. To test the importance of the sterol intermediates, we used *L. major* promastigotes deficient in sterol methyltransferase (*smt*⁻) and C14 demethylase (*c14dm*⁻). Both *smt*⁻ and *c14dm*⁻ have normal sphingolipids but accumulate sterol intermediates instead of ergosterol (25, 26). We challenged

smt⁻ and *c14dm*⁻ promastigotes with SLO. We observed no killing of *smt*⁻ *L. major* promastigotes at doses ≤32,000 HU/ml, despite equivalent binding of toxin (Fig. S3, *A* and *B*). Similarly, we observed no killing of *c14dm*⁻ *L. major* promastigotes at 4000 HU/ml (Fig. S3*C*). We conclude sterol alterations in sphingolipid-deficient *L. major* do not account for the observed cytotoxicity. Instead, sphingolipids protect *L. major* from CDC-mediated cytotoxicity.

One interpretation of sphingolipid-mediated protection is that loss of sphingolipids destabilizes the membrane. While our previous results showing loss of sphingolipids did not

perturb sterol-rich microdomains (7), we tested this hypothesis using detergent challenge of sphingolipid sufficient and deficient cells. If the membrane is broadly destabilized, we predict the cells will be more sensitive to detergents like Triton X-100. When we challenged *L. major* promastigotes with Triton, we found that *c14dm⁻* but neither *spt2⁻*, *c14dm⁻*/+C14DM, nor *spt2⁻*/+SPT2, were more sensitive to detergent than WT promastigotes (Fig. S3D). Thus, we conclude that the sensitivity of sphingolipid-deficient promastigotes is specific to CDCs, and not the result of membrane destabilization.

To control for alternative mechanisms of membrane binding, any impurities in the CDC preparation, and the necessity of pore formation for *L. major* killing, we used three different non-hemolytic SLO mutants. The SLO ΔCRM lacks the cholesterol-binding residues in domain 4 (27). SLO Q476N cannot engage glycans on the cell surface needed for orientation (20, 28). These two mutants do not bind mammalian cells but have no oligomerization or insertion defects (20, 27). If these toxins kill *spt2⁻* and *ipcs⁻ L. major*, it would indicate that SLO can engage *L. major* independently of glycans or sterol. If they fail to kill, it would indicate SLO needs these binding determinants to kill *L. major*. We used a third mutant toxin, SLO ML, which binds but cannot form pores (19, 21). We challenged *spt2⁻* and *ipcs⁻ L. major* with SLO ΔCRM, SLO Q476N, SLO ML or WT SLO (Figs S2, *A* and *C* and S3, *E* and *F*). While SLO WT killed both *spt2⁻* and *ipcs⁻ L. major*, SLO ΔCRM, SLO Q476N, and SLO ML did not (Figs S2, *A* and *C* and S3, *E* and *F*). Similarly, PFO ML failed to kill *spt2⁻* or *ipcs⁻* at all concentrations tested (Fig. S2, *B* and *D*). These data indicate that CDCs require the same binding determinants to target both mammalian membranes and *L. major* membranes.

Since PFO and SLO showed different killing of WT *L. major*, and have distinct membrane binding kinetics, we compared the rate at which SLO and PFO killed sphingolipid-deficient *L. major*. In mammalian cells, SLO more rapidly engages the membrane, whereas PFO binds more slowly (16). Consequently, in HeLa cells there is a larger difference between PFO-mediated killing at 5 min and at 30 min than between SLO-mediated killing (15). We tested the sensitivity of *spt2⁻* or *ipcs⁻ L. major* after 5 min or 30 min of SLO or PFO challenge. For *spt2⁻*, we found that both CDCs had significant changes in LC_{50} between 5 min and 30 min (Figs 2F and S4, *A* and *B*). While the SLO and PFO LC_{50} were similar at 30 min, at 5 min, there was a trend for less killing by PFO compared to SLO (Fig. 2F). We next compared the *spt2⁻* and *ipcs⁻* mutants after CDC challenge. At 5 min, the *ipcs⁻* mutant was killed similarly to *spt2⁻* (Figs. 2G and S4). These data indicate that sterol accessibility is insufficient to determine cytotoxic outcomes in *L. major*. Therefore, to sustain pore formation, SLO and PFO require different lipid environments in the *Leishmania* plasma membrane.

Growth phase of promastigotes does not alter CDC sensitivity

The lipid environment fluctuations during the *L. major* growth cycle could impact CDC sensitivity. The *spt2⁻* promastigotes have defects in phosphatidylethanolamine (PE)

synthesis when their growth reaches the stationary phase (29). In the stationary phase, *L. major* promastigotes differentiate into the infectious metacyclic form over the course of approximately 3 days. We tested the impact of PE defects and metacyclogenesis on CDC killing of *spt2⁻ L. major*. We challenged L. *major* in log phase, or on day 1, 2, or 3 of the stationary phase with 62 to 4000 HU/ml SLO or PFO. At the doses used, SLO and PFO killed *spt2⁻ L. major*, but did not kill wild type or *spt2⁻*/+SPT2 *L. major*, during stationary phase (Figs. 3 and S5, *A–F*). The LC_{50} of SLO and PFO remained similar between log phase and throughout the stationary phase (Figs. 2 and 3), suggesting that changes in PE synthesis did not impact CDC killing of *L. major*. We next determined if the differences we observed for the SLO LC_{50} at 5 min and 30 min in log phase were also present during the stationary phase. The SLO LC_{50} for stationary phase promastigotes changed similarly to log phase (Fig. 3, *B* and *C* and S5, *G–I*). Overall, the sensitivity of *spt2⁻* promastigotes to SLO and PFO did not significantly change during metacyclogenesis, suggesting that changes in PE during growth do not account for CDC sensitivity.

Ceramide may hinder CDC cytotoxicity

One key difference between the *spt2⁻* and *ipcs⁻* that could account for the differences in cytotoxicity is ceramide. The *ipcs⁻* accumulates ceramide because it cannot synthesize it into IPC, whereas the *spt2⁻* cannot synthesize the precursors to ceramide. To determine the contribution of ceramide to CDC cytotoxicity, we used a chemical inhibitor of SPT, myriocin. We treated WT, *spt2⁻*, *spt2⁻*/+SPT2, *ipcs⁻*, and *ipcs⁻*/+IPCS promastigotes with myriocin prior to the CDC challenge. Myriocin increased the SLO sensitivity of wild type and *ipcs⁻*/+IPCS *L. major* similar to that of *spt2⁻*, confirming inhibitor efficacy (Figs. 4 and S6, *A–D*). While sensitized to CDCs, myriocin-treated *spt2⁻*/+SPT2 was more resistant than myriocin-treated WT (Figs. 4 and S6). We attribute this resistance to elevated SPT2 levels in these promastigotes (7). There was no change in the SLO LC_{50} for *spt2⁻* after myriocin treatment, indicating that myriocin was specific for SPT in our assay (Fig. 4). However, the LC_{50} for *ipcs⁻ L. major* decreased 2-fold for SLO and 6-fold for PFO upon myriocin treatment (Figs. 4 and S6). Furthermore, this increase in sensitivity surpassed that of either *spt2⁻* or *ipcs⁻* alone (Figs. 4 and S6). We interpret this finding to suggest that ceramide, which accumulates in *ipcs⁻*, but not *spt2⁻* promastigotes, contributes to protecting the *Leishmania* membrane from damage. Thus, ceramide and other perturbations in the lipid environment might contribute to protection from PFO.

Since PFO showed larger differences in *ipcs⁻* and *spt2⁻* with and without myriocin, we interpret these findings to indicate that PFO is more sensitive to the overall lipid environment in the membrane than SLO. To test this interpretation, we challenged myriocin-treated, *I*nositol phospho*S*phingolipid phospholipase *C-L*ike (ISCL)-deficient (*iscl⁻*) *L. major* with CDCs. *iscl⁻ L. major* lack the lipase that converts IPC back into ceramide, and have elevated IPC levels
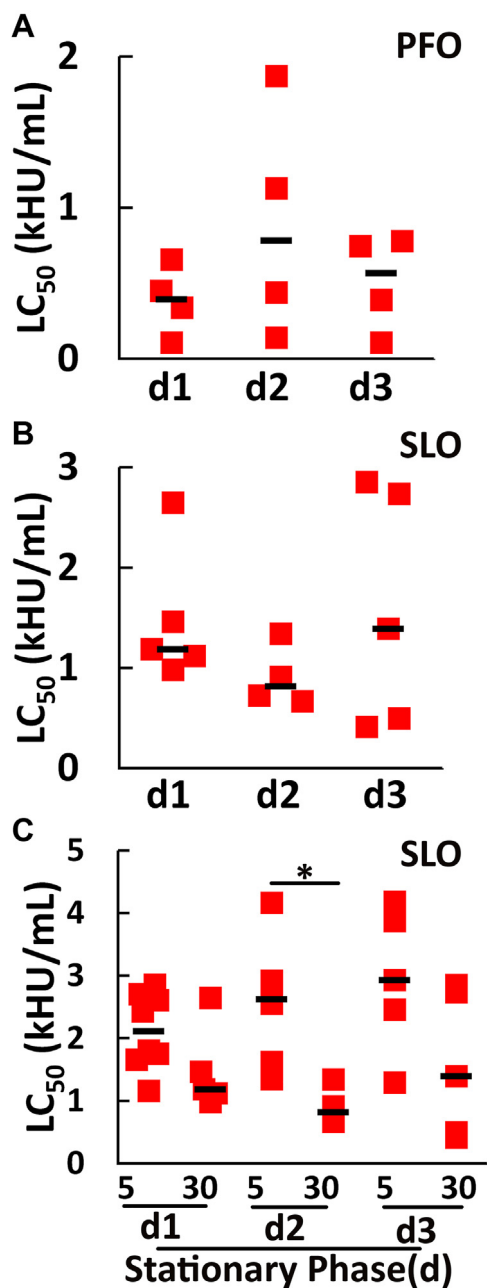
Figure 3. Transition to the stationary phase does not alter CDC sensitivity of *spt2⁻ L. major* promastigotes. *spt2⁻ L. major* promastigotes in each day of the stationary phase were challenged with (*A*) PFO, or (*B* and *C*) SLO for (*A–C*) 30 min or (*C*) 5 min at 37 °C. PI uptake was analyzed by flow cytometry and LC$_{50}$ calculated as described in the methods. Stationary phase d1, d2, and d3 represent 48, 72, and 96 h post log phase. Graphs show individual data points and the median from at least three independent experiments. *p = 0.0145 by one way ANOVA. PFO, perfringolysin O; SLO, Streptolysin O; WT, wild type.

(9). In contrast to myriocin-treated *ipcs⁻ L. major*, which are expected to contain low levels of ceramide, myriocin-treated *iscl⁻ L. major* are expected to contain low levels of IPC. When challenged with SLO or PFO, myriocin-treated *iscl⁻* promastigotes phenocopied myriocin-treated WT promastigotes (Figs. 4, *C* and *D* and S6, *E–H*). Consistent with the primary role of IPC in conferring resistance to cytotoxicity, untreated *iscl⁻* or *iscl⁻/+ISCL L. major* were resistant to SLO

and PFO challenge, even at high toxin doses (Figs. 4, *C* and *D* and S6, *E–H*). Notably, myriocin-treated *ipcs⁻* promastigotes were more sensitive to CDCs compared to WT or *iscl⁻* promastigotes (Figs. 4, *C* and *D* and S6, *E–H*). Overall, these data suggest that IPC provides the most protection against cytotoxicity, but ceramide may also protect *L. major* from the cytotoxicity of pore-forming toxins.

The L3 loop in CDCs senses ceramide in the plasma membrane

We next determined the mechanism by which PFO is more sensitive to ceramide. One key difference between the membrane binding and accessibility of SLO and PFO is the amino acid sequence of the L3 loop (16, 18). These differences in the L3 loop can be switched by single-point mutations. SLO S505D confers PFO-like binding and cytotoxicity on SLO, while PFO D434K has SLO-like binding and cytotoxicity (15, 16, 18). We tested if the cytotoxic differences we observed between CDCs—killing of WT *L. major* at high toxin concentrations and the differences in *spt2⁻* and *ipcs⁻* LC$_{50}$— could be explained by these L3 loop differences. We challenged WT, *spt2⁻*, *ipcs⁻*, and add-back *L. major* promastigotes with PFO, PFO D434K, SLO, or SLO S505D for 30 min. We found that PFO D434K killed WT and *spt2⁻/ +SPT2 L. major* at high concentrations, similar to SLO, while PFO did not kill WT *L. major* or the *spt2⁻/+SPT2* (Fig. 5, *A* and *B*). SLO S505D phenocopied PFO, failing to kill wild type or *spt2⁻/+SPT2 L. major* (Fig. 5, *A* and *B*). While both PFO and PFO D434K killed *spt2⁻ L. major*, SLO S505D was less effective than either PFO or SLO in killing *spt2⁻ L. major* (Fig. 5, *A* and *B*). This is consistent with our previous findings in mammalian cells that SLO S505D has a higher LC$_{50}$ than WT SLO or PFO (15). We repeated these experiments using *ipcs⁻ L. major*. We found broadly similar results with *ipcs⁻* (Fig. 5, *C* and *D*). For each genotype, PFO D434K, with SLO-like binding, was the most potent toxin and showed increased killing even in wild type *L. major* and *ipcs⁻/+IPCS* (Fig. 5E). In contrast, SLO S505D, which has PFO-like binding, had decreased killing (Fig. 5E). We conclude that the differences in SLO and PFO cytotoxicity are due to the differential sensing of ceramide by the L3 loop.

Ceramide and IPC protect L. major *promastigotes from amphotericin B*

Finally, these findings suggest that sphingolipid-deficient *L. major* promastigotes are more sensitive to amphotericin B. We first titrated both myriocin and amphotericin B against WT *L. major* promastigotes to determine the EC$_{50}$. We found myriocin did not inhibit growth more than 25% in promastigotes at 10 μM, while the EC$_{50}$ of amphotericin B was 40 nM (Fig. 6, *A* and *B*). This is similar to the published EC$_{50}$ of amphotericin B, which is 33 nM (30). We next challenged log phase myriocin-treated WT and untreated WT, *spt2*, *spt2/ +SPT2*, *ipcs*, *ipcs/+IPCS* promastigotes with amphotericin B. Removal of both IPC and ceramide increased the sensitivity of *L. major* 2-3-fold, whereas loss of only IPC was not sufficient to increase sensitivity to amphotericin B (Fig. 6, *B–D*). We
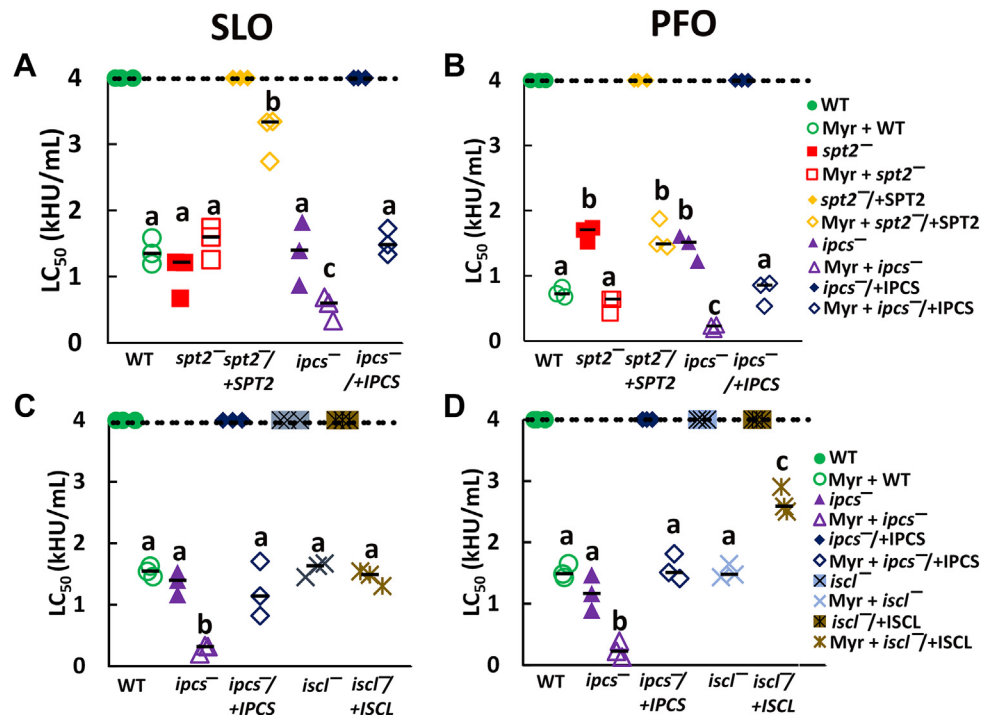
Figure 4. Myriocin treatment of *L. major* promastigotes suggests ceramide helps shield ergosterol. *A* and *B*, WT, *spt2⁻*, spt2⁻/+SPT2, *ipcs⁻* and *ipcs⁻/* +IPCS *L. major* promastigotes grown in either 10 μM myriocin or DMSO supplemented M199 media were challenged with (*A*) SLO or (*B*) PFO for 30 min at 37 °C. *C* and *D*, WT, *iscl⁻*, *iscl⁻/+*ISCL, *ipcs⁻*, and *ipcs⁻/+*IPCS *L. major* promastigotes grown in either 10 μM Myriocin or DMSO supplemented M199 media were challenged with (*C*) SLO or (*D*) PFO for 30 min at 37 °C. PI uptake was analyzed by flow cytometry and LC₅₀ calculated as described in the methods. WT, *ipcs⁻*, and *ipcs⁻/+*IPCS represent distinct assays in each panel. Graphs display medians from three independent experiments. The dashed line indicates the highest concentration used. Points on this line had a LC₅₀ value ≥4000 HU/ml. Statistical significance was determined by one-way ANOVA with Tukey post-testing. Groups sharing the same letter were not statistically different. Myr, myriocin; PFO, perfringolysin O; SLO, Streptolysin O; WT, wild type.

conclude that both ceramide and IPC are needed to protect *L. major* promastigotes from amphotericin B.

Based on these data, we propose a new model of CDC engagement with the *Leishmania* membrane. CDCs are able to bind to the membrane, independently of sphingolipids (Fig. 7). In the absence of sphingolipids, both SLO and PFO oligomerize and insert into the membrane to kill the cell (Fig. 7). The presence of ceramide without IPC provides limited protection against PFO, but not SLO. Recognition of ceramide in this environment is controlled by the L3 loop. Similarly, when Leishmania has its full complement of sphingolipids, ceramide precludes PFO toxicity at high doses but not SLO (Fig. 7). At lower toxin concentrations, however, the sphingolipids prevent toxin insertion by both CDCs.

Discussion

Here we used the human pathogen *L. major* as a medically relevant model organism to understand toxin-membrane interactions. In contrast to mammalian systems, we found that *Leishmania* sphingolipids do not preclude CDC binding to sterols in the membrane, yet still interfere with cytotoxicity. Interference in toxicity was predominantly due to IPC. We further propose a mechanism where ceramide acts as one lipid to selectively reduce PFO, but not SLO, cytotoxicity in cells due to toxin binding determinants in the L3 loop. Disruption of both IPC and ceramide increased the sensitivity of *L. major*

to the anti-*Leishmania* drug amphotericin B. These data show that IPC and ceramide protect *L. major* from ergosterol-binding, pore-forming toxins. This study opens new horizons for future work on membrane repair in *Leishmania* and the competition between bacteria and *L. major*.

We found that Leishmania sphingolipids do not shelter ergosterol from CDCs. Ergosterol may not be sheltered from CDCs by IPC due to structural differences between sphingomyelin and IPC. Based on the crystal structure of the sphingomyelin/cholesterol-binding ostreolysin A and docking models with sphingomyelin, the choline headgroup flexibly lies across the membrane when sphingomyelin is complexed with cholesterol (31). In contrast, the inositol headgroup of IPC is unlikely to adopt this conformation. This could account for the inability of IPC to prevent CDC binding to ergosterol.

We also considered the possibility that sphingolipid perturbations altered sterols, and altered sterols were responsible for the observed phenotypes. A previous study (22) reported that *spt2⁻* promastigotes have lower ergosterol levels, and higher cholesterol levels. While we confirmed an increase in cholesterol and other sterol species with both genetic and chemical inhibition of SPT, we suggest this increase did not impact CDC binding or cytotoxicity. We observed no difference in CDC binding, suggesting that any sterol level alterations were insufficient to change CDC binding to the membrane. Since cholesterol is also involved in pore-formation (32), we tested *L. major* promastigotes lacking
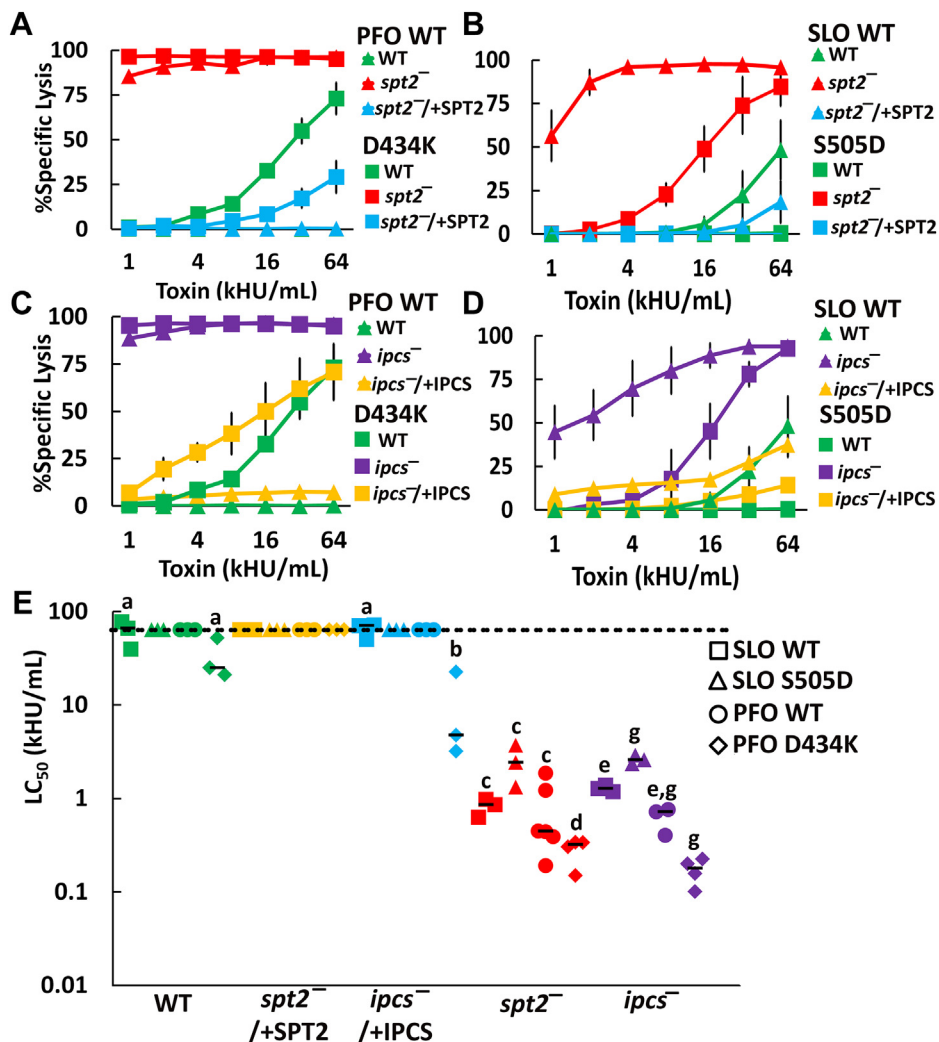
Figure 5. The CDC L3 loop controls CDC cytotoxicity against *L. major* promastigotes. *A* and *B*, WT, *spt2⁻*, and *spt2⁻*/+SPT2 or (*C* and *D*) WT, *ipcs⁻*, and *ipcs⁻*/+IPCS *Leishmania major* promastigotes were challenged with (*A* and *C*) PFO WT, PFO D434K, (*B* and *D*) SLO WT, or SLO S505D at the indicated concentrations for 30 min at 37 °C. PI uptake was analyzed by flow cytometry and (*E*) LC₅₀ calculated as described in the methods. *A–D*, Graphs display the mean ± SEM of at least three independent experiments. *E*, Graph displays individual data points and median from at least three independent experiments. The dashed line indicates the highest concentration used. Points on this line had a LC₅₀ value ≥64,000 HU/ml. Both *spt2⁻* and *ipcs⁻* were statistically significant compared to WT or *ipcs⁻*/+IPCS by 2-way ANOVA. Statistical significance was determined by one-way ANOVA with Tukey post-testing. Within the same genotype, groups sharing the same letter were not statistically different. *A–D*, The x-axis is a log₂ scale. *E*, The y-axis is a log₁₀ scale. CDC, cholesterol-dependent cytolysins; PFO, perfringolysin O; SLO, Streptolysin O; WT, wild type.

SMT and C14DM (25, 26). Both *smt⁻* and *c14dm⁻* have elevated total sterols, and accumulate cholesterol-type sterols, yet were not killed by SLO. Based on these considerations, we conclude that IPC and ceramide are primary determinants for CDC cytotoxicity, but not binding, to *Leishmania* membranes.

The failure to prevent binding by CDCs may represent different physiologic needs of *L. major* and mammalian cells. Mammalian cells need to sense sterol levels provided exogenously by the organism to modify sterol synthesis (5), promote cellular signaling, and endocytosis (33–35). In contrast, *Leishmania* promastigotes are free-swimming organisms that synthesize their own sterols. Furthermore, no clear homologs of the sterol synthesis regulators sterol regulatory element-binding proteins (SREBP) or SREBP cleavage-activating protein have been detected in *Leishmania*. The lack of complications from SREBP signaling represents one advantage to

using *Leishmania* as a model organism to understand sterol membrane dynamics.

While changes in *Leishmania* sphingolipid status did not interfere with CDC binding, changes in both IPC and ceramide reduced the ability of CDCs to kill *L. major*. This finding adds to the controversial role of sphingomyelin and ceramide in preventing *versus* accentuating damage in mammalian cells. On one hand, the sphingomyelinase/pore-forming toxin combination is evolutionarily conserved from bacteria like *C. perfringens* up to venoms in bees and snakes, suggesting that destroying sphingomyelin enhances toxicity. On the other hand, acid sphingomyelinase (36) and/or neutral sphingomyelinase (6) have been reported to promote membrane repair. In mammals, it is not possible to separate the effects of sphingomyelin on cholesterol accessibility from the effects of sphingomyelin on directly interfering with CDC pore
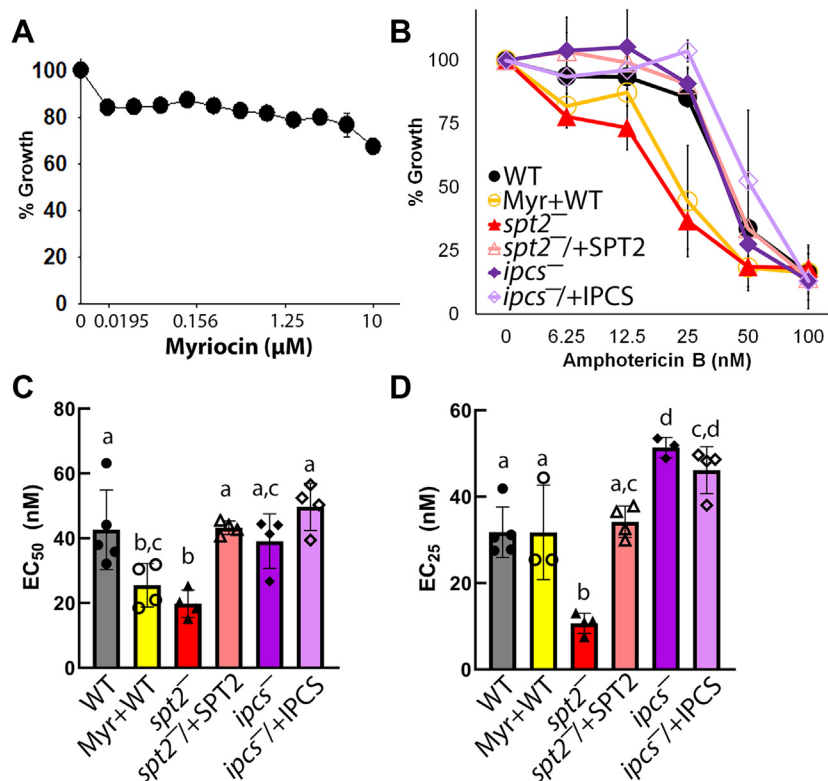
Figure 6. Ceramide protects *L. major* promastigotes from amphotericin B. *A*, WT *L. major* promastigotes were challenged with the indicated concentrations of myriocin and growth determined relative to untreated. *B*, Untreated WT, *spt2⁻*, and *spt2⁻/+SPT2, ipcs⁻,ipcs⁻/+IPCS* or 10 µM myriocin-treated WT *L. major* promastigotes were challenged with the indicated concentration of amphotericin B and growth determined relative to untreated WT. The (*C*) EC_{50} and (*D*) EC_{25} were calculated by logistic regression. Graphs display the mean ± SEM of three independent experiments. Statistical significance was determined by one-way ANOVA. Statistical significance ($p < 0.05$) was assessed by post-hoc testing between groups. Statistical significance was determined by one-way ANOVA with Tukey post-testing. Groups sharing the same letter were not statistically different. *A* and *B*, The x-axis is a $\log_2$ scale. Myr, myriocin; WT, wild type.

formation. Since IPC does not shelter sterol, we were able to determine that IPC interferes with pore formation after binding. We conclude that sphingolipids comprise one key component of the non-permissive membrane environment in *Leishmania* that reduces CDC pore-formation.

We used differences in SLO and PFO binding to mechanistically probe the non-permissive environment. SLO binds rapidly to membranes, whereas PFO requires more time (16). This time difference is reflected in kinetic differences for PFO, but not SLO, cytotoxicity (15). Like mammalian cells, we observed kinetic differences in CDC cytotoxicity in *L. major*. Importantly, PFO was unable to find an environment to promote pore formation in *L. major*, even at supraphysiologic doses. This phenotype was reversed by point mutations in the L3 loop that switch the membrane specificity between PFO and SLO. Since PFO D434K regained the ability to kill WT *L. major*, we conclude that this part of the L3 loop discriminates IPC and/or ceramide. Our findings support the idea that the L3 loop promotes membrane binding, and controls the lipid environment needed for pore formation (16). If the L3 loop also discriminates sphingomyelin in mammalian cells remains to be determined.

Ceramide may modulate CDC cytotoxicity in *L. major*. We found significant differences between the extent of cytotoxicity in the *spt2⁻* and *ipcs⁻*, both of which lack IPC. We found that

this difference was more pronounced when we blocked SPT with myriocin in the *ipcs⁻*, although myriocin treatment phenocopied the *spt2⁻* in our system. The key difference in IPC blockade is that SPT is upstream of ceramide synthesis, whereas IPCS is downstream of ceramide. We suggest that IPC is more protective than ceramide, but ceramide also enhances protection. This contrasts with findings that the addition of ceramide to liposomes containing 35% cholesterol increased membrane permeability to SLO (37). The differences may be due to the system used, protection *via* a ceramide-lipid/protein complex absent in liposomes, changes in membrane fluidity that permits CDC sensing of other lipids, or lipid packing or membrane architecture could be disrupted by sphingolipid or ceramide loss. One argument against these changes driving our observed phenotypes is previous work shows the proportion of detergent-resistant membranes and global membrane architecture is unchanged in *spt2⁻ L. major* (7, 38). This suggests membrane architecture is broadly preserved. Second, binding did not change, which suggests loss of sphingolipids did not increase the extent of toxin binding. Overall, we propose that ceramide is one lipid species sensed by CDCs when forming pores in membranes.

While we showed that *Leishmania* sphingolipids limit cytotoxicity, but not binding, our study had limitations that can be explored in future studies. We did not determine the
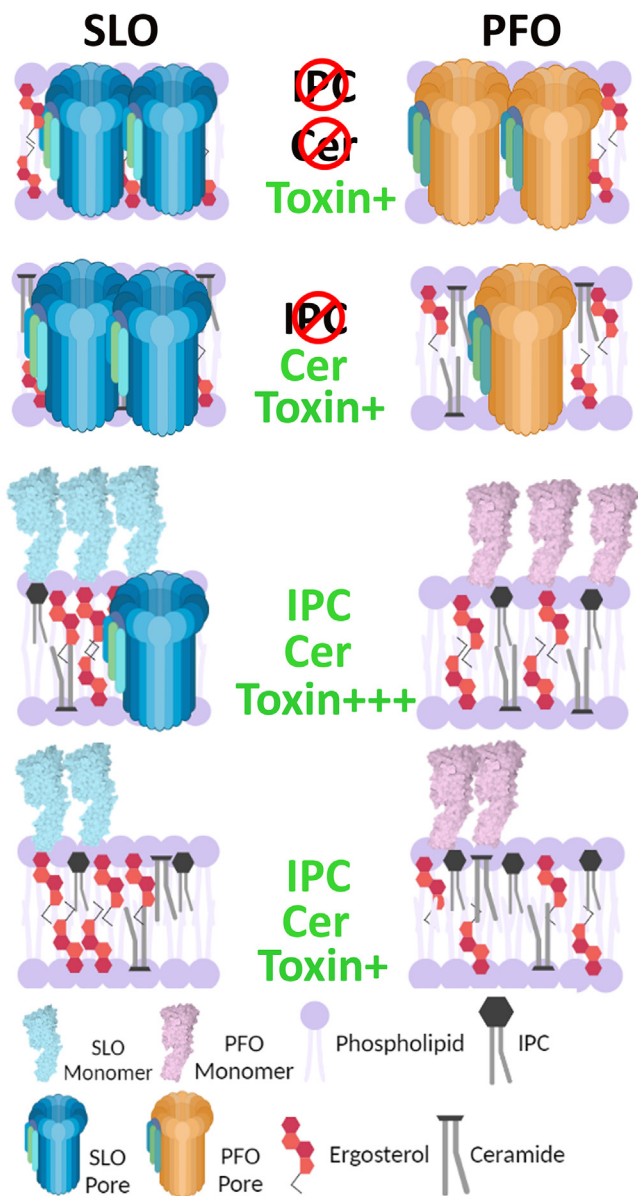
Figure 7. Cytotoxicity of CDCs toward *L. major* promastigotes is dependent on the presence of IPC. CDCs can bind to ergosterol in the membrane of *L. major* promastigotes regardless of sphingolipids. In the absence of IPC and ceramide, both SLO and PFO form lytic pores in the membrane. Elimination of IPC, but not ceramide, favors SLO pore formation but reduced PFO pore formation. In the presence of ceramide and IPC, only SLO can still form pores at high doses (Toxin+++). At lower toxin doses (Toxin+), neither toxin can form pores in the membrane. The displayed inner-outer leaflet distributions of ergosterol and ceramide are for illustrative purposes only because the relative distribution of these lipids between inner and outer leaflets in *L. major* promastigotes is currently unknown. CDC, cholesterol-dependent cytolysins; IPC, inositol phosphorylceramide; PFO, perfringolysin O; SLO, Streptolysin O.

total fraction of plasma membrane ergosterol needed to support lysis by CDCs. In mammals, the binding of inactive CDCs was used to probe the proportion of cholesterol in the membrane (5), though the smaller size of *Leishmania* makes this more challenging to detect. Instead, we focused on comparing the accessible pool of sterol with the sphingolipid-sheltered pool of sterol in *Leishmania*. While we interpret our binding data to indicate sphingolipids do not protect ergosterol, an

essential pool of ergosterol could exist that is bound to other proteins and/or lipids. We did not use a mouse model. The high efficacy of the single agents in the mouse model makes detecting synergistic effects from combination therapy there challenging.

We did not examine amastigotes because they salvage lipids from the host macrophage (39–41), the membranes are substantially similar in *spt2*⁻, *ipcs*⁻, and WT amastigotes (12, 42), and contaminating macrophage membranes could obscure results. Future work is needed to determine how salvaged lipids impact sphingolipid-deficient *Leishmania* survival. Since CDC-producing Gram-positive bacteria, including *S. pyogenes*, contribute to secondary bacterial infections during cutaneous leishmaniasis (43, 44), CDCs could contribute to late-stage infection, and/or the time required for resolution. Similarly, our work provides a foundation for understanding the competition in the sandfly midgut between bacteria-producing, pore-forming toxins and *L. major* in the sandfly midgut.

Overall, we established *L. major* as a pathogenically relevant and genetically tractable model system for studying biological membranes and identified key differences in sterol/sphingolipid organization compared to mammalian cells. Most prior membrane biology work was done either in opisthokonts or in model liposomes, so there are few studies on biological membranes in other taxonomic groups, including human pathogens. We provide a blueprint for examining the membranes of non-standard organisms. These findings provide important perspectives for the generalization of biological membranes, especially compared to opisthokonts.

Experimental procedures

Reagents

All reagents were from Thermofisher Scientific unless otherwise noted. Cysteine-less His-tagged PFO (PFO WT) in pET22 was a generous gift from Rodney Tweten (University of Oklahoma Health Sciences Center). Cysteine-less, codon-optimized SLO (SLO WT) in pBAD-gIII was synthesized at Genewiz. The C530A mutant retains WT binding, hemolytic activity, and pore structure, but it is redox resistant (45). Monomer-locked (G398V/G399V) SLO, cysteine-less SLO (C530A), SLO S505D, and PFO D434K were previously described (15, 21). Glycan-binding (SLO Q476N) (20) and cholesterol-binding (SLO T564A/L565A) (SLO ΔCRM) SLO mutants (27) and ML (G298V/G299V) PFO mutants were generated using Quikchange PCR and verified by Sanger sequencing. Primer sequences are available upon request.

Recombinant toxins

Toxins were induced and purified as previously described (21, 46). Toxins were induced with 0.2% arabinose (SLO WT, SLO S505D, SLO G398V/G399V, SLO Q476N, SLO T564A/L565A (ΔCRM)), or 0.2 mM IPTG (PFO, PFO D434K, and PFO G298V/G299V) for 3 h at room temperature and purified using Nickel-NTA beads. For Cy5 conjugation, recombinant

toxins were gel filtered into 100 mM sodium bicarbonate (pH 8.5) using a Zeba gel filtration column according to the manufacturer's instructions. Enough Cy5 monoreactive dye (GE Healthcare) to label 1 mg protein was added to 3 to 4 mg toxin and incubated overnight at 4 °C. Conjugated toxins were gel filtered into PBS to remove unconjugated Cy5 dye, aliquoted, and snap-frozen in dry ice. Protein concentration was determined by Bradford assay and hemolytic activity was determined as previously described (15) using human red blood cells (Zen Bio). One hemolytic unit is defined as the amount of toxin required to lyse 50% of a 2% human red blood cell solution in 30 min at 37 °C in 2 mM CaCl₂, 10 mM HEPES, pH 7.4, and 0.3% BSA in PBS. The specific activities of SLO monomer-locked Cy5 and PFO monomer-locked Cy5 were <10 HU/mg. They were used at a mass equivalent to wild-type SLO and PFO. Multiple toxin preparations were used (Table 2).

Leishmania strains and culture

LV39 clone 5 (Rho/SU/59/P) was used as the WT strain, and all genetic mutants were made in this background. The serine palmitoyl transferase subunit 2 knockout Δspt2::HYG/Δspt2::PAC (spt2⁻), episomal addback Δspt2::HYG/Δspt2:PAC/+pXG-SPT2 (spt2⁻/+SPT2) (7), the inositol phosphosphingolipid phospholipase C-like knockout Δiscl2::HYG/Δiscl2::PAC (iscl⁻), episomal addback Δiscl2::HYG/Δiscl2::PAC/+pXG-ISCL (iscl⁻/+ISCL) (47), sterol methyltransferase knockout Δsmt::HYG/Δsmt::PAC (smt⁻) (25), episomal addback Δsmt::HYG/Δsmt::PAC/+pXG-SMT (smt⁻/+SMT) (25), sterol 14-α- demethylase knockout Δc14dm:HYG/Δc14dm::PAC (c14dm⁻) (26), and episomal addback Δc14dm:HYG/Δc14dm::PAC/+pXG-C14DM (c14dm⁻/+C14DM) (26) have been previously described. The IPC synthase knockout Δipcs::HYG/Δipcs::PAC (ipcs⁻) and episomal addback Δipcs::HYG/Δipcs::PAC/+pXG-IPCS (ipcs⁻/+IPCS) were generated in the Beverley lab (12). Elevation of ceramide levels and lack of IPC were confirmed by mass spectrometry (12). Wild type L. *major* LV39, spt2⁻, ipcs⁻, smt⁻, and iscl⁻ were cultured at 27 °C in M199 medium with 0.182% NaHCO₃, 40 mM Hepes, pH 7.4, 0.1 M adenine, 1 μg/ml biotin, 5 μg/ml hemin & 2 μg/ml biopterin and 10% heat-inactivated fetal bovine serum, pH 7.4. Episomal addback cells spt2⁻/+SPT2, ipcs⁻/+IPCS, smt⁻/+SMT, and iscl⁻/+ISCL were maintained in complete medium in the presence of 10 μg/ml neomycin (G418) and 20 μg/ml blasticidin, except experimental passages. Leishmania strains were cryopreserved, and the lack of sphingolipids validated by mass spectrometry (Fig. S7).

Culture density and cell viability were determined by hemocytometer counting and flow cytometry after propidium iodide staining at a final concentration of 20 μg/ml. In this study, log phase promastigotes refer to replicative parasites at 2.0 to 8.0 × 10⁶ cells/ml, and stationary phase promastigotes referred to non-replicative parasites at densities higher than 2.0 × 10⁷ cells/ml. Cells are considered Stationary Day 0 when they reach 2.0 x10⁷ cells/ml. They are Stationary Day 1, Stationary Day 2 and Stationary Day 3 at 24, 48, 72 h after they reach Stationary Day 0, respectively.

Drug treatment of L. major

For myriocin treatment, experimental log phase cells were seeded at 1.0 × 10⁵ cells/ml in complete medium and either treated with 10 μM Myriocin dissolved in 1X DMSO (experimental) or an equivalent volume of diluent 1× DMSO (control). Cells were cultured and allowed to reach the log phase in 48 h before harvesting and processing cells for experiments. For amphotericin B, log phase L. *major* promastigotes were inoculated in complete M199 media at 2.0 × 10⁵ cells/ml in 0 to 100 nM of amphotericin B. Culture densities were measured after 48 h of incubation in 24-well plates. EC₅₀ and EC₂₅ were determined by logistic regression using cells grown in the absence of amphotericin B as controls.

Leishmania processing for experiments

Cells were cultured in complete medium to log phase or stationary phase, according to experimental requirements. Cells were counted and centrifuged at 3200 RPM (Rotor SX4750), 8 min to pellet cells at room temperature (25 °C). Cells were washed with 1X PBS and counted again for accuracy. Cells were centrifuged at 3200 RPM (Rotor SX4750), 8 min to pellet cells at room temperature (25 °C), and resuspended in serum-free 1X M199 to a final concentration of 1.0 × 10⁶ cells/ml. Thus, 100 μl of cells used per sample/well in 96 well plates contained 1.0 × 10⁵ cells.

HeLa cell culture

HeLa cells (ATCC CCL-2) were maintained at 37 °C, 5% CO₂ in DMEM (Corning, Corning, NY, USA) supplemented with 10% Equafetal bovine serum (Atlas Biologicals, Fort Collins, CO, USA) and 1 × L-glutamine (D10). They were negative for *Mycoplasma* by microscopy.

Table 2
Specific activity of active toxin preparations used

Toxin	Figure Used	Specific activity (HU/mg)
SLO WT	2A, 2C, 2E, S2C	1.23×10^6
	2E, S2A, S2F	8.3×10^4
	2F, 2G, S4	1.42×10^5
	3B, S5D-F	3.4×10^5
	3C, S5G-I	1.11×10^5
	4, S6	3.3×10^5
	5	3.3×10^5
	S1	4.92×10^5
	S2E	1.2×10^6
	S3B	3.77×10^5
	S3C	4.81×10^5
	S3E-F	2×10^5
SLO S505D	5	3.95×10^4
PFO D434K	5	7.87×10^6
PFO WT	2B, 2D, S2D	8.39×10^6
	2F, S2B, S2F	2.73×10^4
	2F, S4	1.92×10^5
	2E	1.63×10^5
	2G, S4, 4, S6	3.63×10^5
	3, S5	4.57×10^6
	5	1.75×10^6

🔹ASBMB

J. Biol. Chem. (2023) 299(6) 104745 **11**

Sphingolipids protect Leishmania

Binding assay with L. major promastigotes L. major

Promastigotes were resuspended at 1×10^6 cells/ml in M199 media supplemented with 2 mM $CaCl_2$ and 20 μg/ml propidium iodide. Cy5-conjugated toxins were diluted in serum-free M199 media according to a mass equivalent to the active toxin and further diluted in two-fold intervals. Cells were examined for PI and Cy5 fluorescence using an Attune flow cytometer. Debris was gated out and cells exhibiting high PI fluorescence (1–2 log shift) (PI high), low PI fluorescence (∼1 log shift) (PI low) or background PI fluorescence (PI neg) were quantified, normalized against untreated cells and graphed according to mass used for inactive toxin (Fig. S1, *B* and *C*). Both PI neg and PI low populations remain metabolically active, indicating that only the PI high population are dead cells (23). The median fluorescence intensity (MFI) of Cy5 labeled, PI-negative population was quantified, background-subtracted using cells receiving no Cy5-conjugated toxin. MFI was plotted against mass of inactive Cy5-conjugated toxin (SLO ML or PFO ML). To normalize binding to the surface area, we assumed HeLa cells in suspension were spheres of radius 7.5 μm, while *L. major* promastigotes were ellipsoids with a major radius 5 μm and minor radii 1.25 μm. The ellipsoid surface area was calculated using the Knud-Thompson formula. The MFI was divided by the final calculated surface area and reported as normalized MFI (Fig. S1*A*).

Flow cytometry cytotoxicity assay with L. major promastigotes

Killing assays were performed as described (48). *L. major* promastigotes were resuspended at 1×10^6 cells/ml in M199 media supplemented with 2 mM $CaCl_2$ and 20 μg/ml propidium iodide. HeLa cells were resuspended at 1×10^6 cells/ml in RPMI media supplemented with 2 mM $CaCl_2$ and 20 μg/ml propidium iodide. Toxins were diluted in serum-free M199 media for *Leishmania* promastigotes or in serum-free RPMI media for HeLa cells according to hemolytic activity (wild-type toxins) or equivalent mass (inactive mutant toxins) and further diluted in twofold intervals. PI fluorescence in cells was measured using an Attune flow cytometer. Debris was gated out and cells exhibiting high PI fluorescence (1–2 log shift) (PI high), low PI fluorescence (∼1 log shift) (PI low), or background PI fluorescence (PI neg) were quantified, normalized against untreated cells and graphed according to toxin concentration (Fig. S1). Specific lysis was determined as follows: % Specific Lysis = (% PI High^{Experimental} - % PI High^{Control})/(100− %PI High^{Control}). The sublytic dose was defined as the highest toxin concentration that gave <20% specific lysis.

MTT assay

The MTT assay was performed as described (15) with the following modifications. *L. major* promastigotes were resuspended at 2.5×10^7 cells/ml in phenol red-free DMEM supplemented with 2 mM $CaCl_2$. Toxins were diluted in serum-free, phenol red-free DMEM according to hemolytic activity and further diluted in twofold intervals. In each well, 2.5×10^6 cells were incubated with toxin for 30 min at 37 °C, washed, and incubated with 1.2 mM MTT reagent in phenol red-free DMEM for 4 h at 37 °C. Formazan was solubilized overnight with SDS-HCl. Plates were read at A_{450}. The % viability was determined as (A_{450}xpt – background)/ (A_{450}control – background) × 100%. The specific lysis was calculated as 100 – % viability. The LC_{50} was determined from specific lysis curves using linear regression.

Sterol analysis by gas chromatography/mass spectrophotometry (GC-MS)

Total lipids were extracted according to a modified Folch's protocol (49). *L. major* promastigotes (DMSO treated or treated with 10 μM myriocin for 48 h first) were resuspended in chloroform: methanol (2:1) at 1.0×10^8 cells/ml along with the internal standard cholesta-3,5-diene [(FW = 368.84) from Avanti Polar Lipids] at 2.0×10^7 molecules/cell and vortexed for 30 s. Cell debris was removed by centrifugation (2500 RPM/1000*g* for 10 min) and the supernatant was washed with 0.2 volume of 1X PBS. After centrifugation, the aqueous layer was removed and the organic phase was dried under a stream of N_2 gas. Lipid samples were then dissolved in methanol at the equivalence of 1.0×10^9 cells/ml. An internal standard, cholesta-3,5-diene (formula weight, 368.34), was provided at 2.0×10^7 molecules/cell during extraction. For GC-MS, equal amounts of lipid extract were transferred to separate vial inserts, evaporated to dryness under nitrogen, and derivatized with 50 μl of N,O-Bis(trimethylsilyl)trifluoroacetamide plus 1% trimethylchlorosilane in acetonitrile (1:3), followed by heating at 70 °C for 30 min. GC-MS analysis was conducted on an Agilent 7890A GC coupled with Agilent 5975C MSD in electron ionization mode. Derivatized samples (2 μl each) were injected with a 10:1 split into the GC column with the injector and transfer line temperatures set at 250 °C. The GC temperature started at 180 °C and was held for 2 min, followed by 10 °C/min increase until 300 °C and then held for 15 min. To confirm that the unknown GC peak retention time matched that of the episterol standard, we also used a second temperature program started at 80 °C for 2 min, ramped to 260 °C at 50 °C/min, held for 15 min, and increased to 300 °C at 10 °C/min and held for 10 min. A 25-m Agilent J & W capillary column (DB-1; inner diameter, 0.25 mm; film thickness, 0.1 μm) was used for the separation.

PE and sphingolipid analysis by electrospray mass spectrometry

To analyze the relative abundance of PE and sphingolipids, parasite lipids were extracted using the Bligh–Dyer approach (50) and examined by electrospray mass spectrometry in the negative ion mode as previously described (51).

Statistics

Prism (Graphpad), Sigmaplot 11.0 (Systat Software Inc, San Jose, CA), or Excel were used for statistical analysis. Data are represented as mean ± SEM as indicated. The LC_{50} for toxins

was calculated by linear regression of the linear portion of the death curve. Statistical significance was determined either by one-way ANOVA with Tukey post-testing, one-way ANOVA (Brown-Forsythe method) with Dunnett T3 post-testing, or Kruskal-Wallis, as appropriate. $P < 0.05$ was considered to be statistically significant. Graphs were generated in Excel and Photoshop (Adobe).

Data availability

All data are available in the main text or the supplementary materials.

References

1. Baginski, M., and Czub, J. (2009) Amphotericin B and its new derivatives - mode of action. *Curr. Drug Metab.* **10**, 459–469
2. Alpizar-Sosa, E. A., Ithnin, N. R. B., Wei, W., Pountain, A. W., Weidt, S. K., Donachie, A. M., *et al.* (2022) Amphotericin B resistance in leishmania mexicana: alterations to sterol metabolism and oxidative stress response. *PLoS Negl. Trop. Dis.* **16**, e0010779
3. Berman, J. (2003) Current treatment approaches to leishmaniasis. *Curr. Opin. Infect. Dis.* **16**, 397–401
4. Coukell, A. J., and Brogden, R. N. (1998) Liposomal amphotericin B. Therapeutic use in the management of fungal infections and visceral leishmaniasis. *Drugs* **55**, 585–612
5. Das, A., Brown, M. S., Anderson, D. D., Goldstein, J. L., and Radhakrishnan, A. (2014) Three pools of plasma membrane cholesterol and their relation to cholesterol homeostasis. *Elife* **3**, e02882
6. Schoenauer, R., Larpin, Y., Babiychuk, E. B., Drucker, P., Babiychuk, V. S., Avota, E., *et al.* (2019) Down-regulation of acid sphingomyelinase and neutral sphingomyelinase-2 inversely determines the cellular resistance to plasmalemmal injury by pore-forming toxins. *FASEB J.* **33**, 275–285
7. Zhang, K., Showalter, M., Revollo, J., Hsu, F. F., Turk, J., and Beverley, S. M. (2003) Sphingolipids are essential for differentiation but not growth in Leishmania. *EMBO J.* **22**, 6016–6026
8. Zhang, K., and Beverley, S. M. (2010) Phospholipid and sphingolipid metabolism in Leishmania. *Mol. Biochem. Parasitol.* **170**, 55–64
9. Zhang, O., Wilson, M. C., Xu, W., Hsu, F. F., Turk, J., Kuhlmann, F. M., *et al.* (2009) Degradation of host sphingomyelin is essential for Leishmania virulence. *Plos Pathog.* **5**, e1000692
10. Sepcic, K., Berne, S., Rebolj, K., Batista, U., Plemenitas, A., Sentjurc, M., *et al.* (2004) Ostreolysin, a pore-forming protein from the oyster mushroom, interacts specifically with membrane cholesterol-rich lipid domains. *FEBS Lett.* **575**, 81–85
11. Yamaji, A., Sekizawa, Y., Emoto, K., Sakuraba, H., Inoue, K., Kobayashi, H., *et al.* (1998) Lysenin, a novel sphingomyelin-specific binding protein. *J. Biol. Chem.* **273**, 5300–5306
12. Kuhlmann, F. M., Key, P. N., Hickerson, S. M., Turk, J., Hsu, F. F., and Beverley, S. M. (2022) Inositol phosphorlyceramide synthase null Leishmania are viable and virulent in animal infections where salvage of host sphingomyelin predominates. *J. Biol. Chem.* **298**, 102522
13. Thapa, R., Ray, S., and Keyel, P. A. (2020) Interaction of macrophages and cholesterol-dependent cytolysins: the impact on Immune response and cellular survival. *Toxins (Basel)* **12**, 531
14. Savinov, S. N., and Heuck, A. P. (2017) Interaction of cholesterol with perfringolysin O: what have we learned from functional analysis? *Toxins (Basel)* **9**, 381
15. Ray, S., Thapa, R., and Keyel, P. A. (2018) Multiple parameters beyond lipid binding affinity drive cytotoxicity of cholesterol-dependent Cytolysins. *Toxins (Basel)* **11**, 1
16. Farrand, A. J., Hotze, E. M., Sato, T. K., Wade, K. R., Wimley, W. C., Johnson, A. E., *et al.* (2015) The cholesterol-dependent cytolysin membrane-binding interface discriminates lipid environments of cholesterol to support beta-barrel pore insertion. *J. Biol. Chem.* **290**, 17733–17744
17. Hotze, E. M., Heuck, A. P., Czajkowsky, D. M., Shao, Z., Johnson, A. E., and Tweten, R. K. (2002) Monomer-monomer interactions drive the prepore to pore conversion of a beta-barrel-forming cholesterol-dependent cytolysin. *J. Biol. Chem.* **277**, 11597–11605
18. Johnson, B. B., Moe, P. C., Wang, D., Rossi, K., Trigatti, B. L., and Heuck, A. P. (2012) Modifications in perfringolysin O domain 4 alter the cholesterol concentration threshold required for binding. *Biochemistry* **51**, 3373–3382
19. Magassa, N., Chandrasekaran, S., and Caparon, M. G. (2010) Streptococcus pyogenes cytolysin-mediated translocation does not require pore formation by streptolysin O. *EMBO Rep.* **11**, 400–405

20. Mozola, C. C., and Caparon, M. G. (2015) Dual modes of membrane binding direct pore formation by Streptolysin O. *Mol. Microbiol.* **97**, 1036–1050

21. Romero, M., Keyel, M., Shi, G., Bhattacharjee, P., Roth, R., Heuser, J. E., *et al.* (2017) Intrinsic repair protects cells from pore-forming toxins by microvesicle shedding. *Cell Death Differ.* **24**, 798–808

22. Armitage, E. G., Alqaisi, A. Q. I., Godzien, J., Pena, I., Mbekeani, A. J., Alonso-Herranz, V., *et al.* (2018) Complex interplay between sphingolipid and sterol metabolism revealed by perturbations to the leishmania Metabolome caused by miltefosine. *Antimicrob. Agents Chemother.* **62**, e02095–e02117

23. Keyel, P. A., Loultcheva, L., Roth, R., Salter, R. D., Watkins, S. C., Yokoyama, W. M., *et al.* (2011) Streptolysin O clearance through sequestration into blebs that bud passively from the plasma membrane. *J. Cell Sci* **124**, 2414–2423

24. Ray, S., Roth, R., and Keyel, P. A. (2022) Membrane repair triggered by cholesterol-dependent cytolysins is activated by mixed lineage kinases and MEK. *Sci. Adv.* **8**, eabl6367

25. Mukherjee, S., Xu, W., Hsu, F. F., Patel, J., Huang, J., and Zhang, K. (2019) Sterol methyltransferase is required for optimal mitochondrial function and virulence in Leishmania major. *Mol. Microbiol.* **111**, 65–81

26. Xu, W., Hsu, F. F., Baykal, E., Huang, J., and Zhang, K. (2014) Sterol biosynthesis is required for heat resistance but not extracellular survival in leishmania. *PLoS Pathog.* **10**, e1004427

27. Farrand, A. J., LaChapelle, S., Hotze, E. M., Johnson, A. E., and Tweten, R. K. (2010) Only two amino acids are essential for cytolytic toxin recognition of cholesterol at the membrane surface. *Proc. Natl. Acad. Sci. U. S. A.* **107**, 4341–4346

28. Shewell, L. K., Day, C. J., Jen, F. E., Haselhorst, T., Atack, J. M., Reijneveld, J. F., *et al.* (2020) All major cholesterol-dependent cytolysins use glycans as cellular receptors. *Sci. Adv.* **6**, eaaz4926

29. Zhang, K., Pompey, J. M., Hsu, F. F., Key, P., Bandhuvula, P., Saba, J. D., *et al.* (2007) Redirection of sphingolipid metabolism toward de novo synthesis of ethanolamine in Leishmania. *EMBO J.* **26**, 1094–1104

30. Seifert, K., and Croft, S. L. (2006) *In vitro* and *in vivo* interactions between miltefosine and other antileishmanial drugs. *Antimicrob. Agents Chemother.* **50**, 73–79

31. Endapally, S., Frias, D., Grzemska, M., Gay, A., Tomchick, D. R., and Radhakrishnan, A. (2019) Molecular discrimination between two conformations of sphingomyelin in plasma membranes. *Cell* **176**, 1040–1053.e17

32. Giddings, K. S., Johnson, A. E., and Tweten, R. K. (2003) Redefining cholesterol's role in the mechanism of the cholesterol-dependent cytolysins. *Proc. Natl. Acad. Sci. U. S. A.* **100**, 11315–11320

33. Rodal, S. K., Skretting, G., Garred, O., Vilhardt, F., van Deurs, B., and Sandvig, K. (1999) Extraction of cholesterol with methyl-beta-cyclodextrin perturbs formation of clathrin-coated endocytic vesicles. *Mol. Biol. Cell* **10**, 961–974

34. Sen, S., Roy, K., Mukherjee, S., Mukhopadhyay, R., and Roy, S. (2011) Restoration of IFNgammaR subunit assembly, IFNgamma signaling and parasite clearance in leishmania donovani infected macrophages: role of membrane cholesterol. *PLoS Pathog.* **7**, e1002229

35. Subramaniam, P. S., and Johnson, H. M. (2002) Lipid microdomains are required sites for the selective endocytosis and nuclear translocation of IFN-gamma, its receptor chain IFN-gamma receptor-1, and the phosphorylation and nuclear translocation of STAT1alpha. *J. Immunol.* **169**, 1959–1969

36. Tam, C., Idone, V., Devlin, C., Fernandes, M. C., Flannery, A., He, X., *et al.* (2010) Exocytosis of acid sphingomyelinase by wounded cells promotes endocytosis and plasma membrane repair. *J. Cell Biol.* **189**, 1027–1038

37. Zitzer, A., Bittman, R., Verbicky, C. A., Erukulla, R. K., Bhakdi, S., Weis, S., *et al.* (2001) Coupling of cholesterol and cone-shaped lipids in bilayers augments membrane permeabilization by the cholesterol-specific toxins streptolysin O and vibrio cholerae cytolysin. *J. Biol. Chem.* **276**, 14628–14633

38. Denny, P. W., and Smith, D. F. (2004) Rafts and sphingolipid biosynthesis in the kinetoplastid parasitic protozoa. *Mol. Microbiol.* **53**, 725–733

39. Henriques, C., Atella, G. C., Bonilha, V. L., and de Souza, W. (2003) Biochemical analysis of proteins and lipids found in parasitophorous vacuoles containing Leishmania amazonensis. *Parasitol. Res.* **89**, 123–133

40. Moitra, S., Basu, S., Pawlowic, M., Hsu, F. F., and Zhang, K. (2021) De novo synthesis of phosphatidylcholine is essential for the promastigote but not amastigote stage in Leishmania major. *Front. cell. infect. microbiol.* **11**, 647870

41. Winter, G., Fuchs, M., McConville, M. J., Stierhof, Y. D., and Overath, P. (1994) Surface antigens of leishmania mexicana amastigotes: characterization of glycoinositol phospholipids and a macrophage-derived glycosphingolipid. *J. Cell Sci.* **107**, 2471–2482

42. Zhang, K., Hsu, F. F., Scott, D. A., Docampo, R., Turk, J., and Beverley, S. M. (2005) Leishmania salvage and remodelling of host sphingolipids in amastigote survival and acidocalcisome biogenesis. *Mol. Microbiol.* **55**, 1566–1578

43. Jayasena Kaluarachchi, T. D., Campbell, P. M., Wickremasinghe, R., Ranasinghe, S., Wickremasinghe, R., Yasawardene, S., *et al.* (2021) Distinct microbiome profiles and biofilms in Leishmania donovani-driven cutaneous leishmaniasis wounds. *Sci. Rep.* **11**, 23181

44. Gimblet, C., Meisel, J. S., Loesche, M. A., Cole, S. D., Horwinski, J., Novais, F. O., *et al.* (2017) Cutaneous leishmaniasis induces a transmissible dysbiotic skin microbiota that promotes skin inflammation. *Cell Host Microbe* **22**, 13–24.e14

45. Keyel, P. A., Roth, R., Yokoyama, W. M., Heuser, J. E., and Salter, R. D. (2013) Reduction of streptolysin O (SLO) pore-forming activity enhances inflammasome activation. *Toxins (Basel)* **5**, 1105–1118

46. Keyel, P. A., Heid, M. E., Watkins, S. C., and Salter, R. D. (2012) Visualization of bacterial toxin induced responses using live cell fluorescence microscopy. *J. Vis. Exp.* , e4227. https://doi.org/10.3791/4227

47. Zhang, O., Xu, W., Balakrishna Pillai, A., and Zhang, K. (2012) Developmentally regulated sphingolipid degradation in Leishmania major. *PLoS One* **7**, e31059

48. Haram, C. S., Moitra, S., Keane, R., Breslav, E., Zhang, K., and Keyel, P. A. (2022) Deciphering the molecular mechanism and function of pore-forming toxins using leishmania major. *J. Vis. Exp.* https://doi.org/10.3791/64341

49. Folch, J., Lees, M., and Sloane Stanley, G. H. (1957) A simple method for the isolation and purification of total lipides from animal tissues. *J. Biol. Chem.* **226**, 497–509

50. Bligh, E. G., and Dyer, W. J. (1959) A rapid method of total lipid extraction and purification. *Can. J. Biochem. Physiol.* **37**, 911–917

51. Pawlowic, M. C., Hsu, F. F., Moitra, S., Biyani, N., and Zhang, K. (2016) Plasmenylethanolamine synthesis in Leishmania major. *Mol. Microbiol.* **101**, 238–249

ASBMB